

1 **Modelling silicon supply during the Last Interglacial (MIS 5e) at Lake Baikal**

2 Panizzo, V.N.^{1,2}, Swann, G.E.A.^{1,2}, Mackay, A.W.³, Pashley, V.⁴, and Horstwood, M.S.A.⁴

3 ¹*School of Geography, University of Nottingham, University Park, Nottingham, NG7 2RD, UK*

4 ²*Centre for Environmental Geochemistry, University of Nottingham, University Park, Nottingham,*
5 *NG7 2RD, UK*

6 ³*Environmental Change Research Centre, Department of Geography, University College London,*
7 *Gower Street, London, WC1E 6BT, UK*

8 ⁴*NERC Isotope Geosciences Laboratory, British Geological Survey, Keyworth, Nottingham, NG12*
9 *5GG, UK*

10

11 *Corresponding author: virginia.panizzo@nottingham.ac.uk

12

13 **Abstract**

14 Limnological reconstructions of primary productivity have demonstrated its response over Quaternary
15 timescales to drivers such as climate change, landscape evolution and lake ontogeny. In particular,
16 sediments from Lake Baikal, Siberia, provide a valuable uninterrupted and continuous sequence of
17 biogenic silica (BSi) records, which document orbital and sub-orbital frequencies of regional climate
18 change. We here extend these records via the application of stable isotope analysis of silica in diatom
19 opal ($\delta^{30}\text{Si}_{\text{diatom}}$) from sediments covering the Last Interglacial cycle (Marine Isotope Stage [MIS] 5e; c.
20 130 to 115 ka BP) as a means to test the hypothesis that it was more productive than the Holocene.
21 $\delta^{30}\text{Si}_{\text{diatom}}$ data for the Last Interglacial range between +1.29 to +1.78‰, with highest values between c.
22 127 to 124 ka BP (+1.57 to +1.78‰). Results show that diatom dissolved silicon (DSi) utilisation, was
23 significantly higher ($p=0.001$) during MIS 5e than the current interglacial, which reflects increased
24 diatom productivity over this time (concomitant with high diatom biovolume accumulation rates
25 [BVAR] and warmer pollen-inferred vegetation reconstructions). Diatom BVAR are used, in tandem
26 with $\delta^{30}\text{Si}_{\text{diatom}}$ data, to model DSi supply to Lake Baikal surface waters, which shows that highest
27 delivery was between c. 123 to 120 ka BP (reaching peak supply at c. 120 ka BP). When constrained
28 by sedimentary mineralogical archives of catchment weathering indices (e.g. the Hydrolysis Index),
29 data highlight the small degree of weathering intensity and therefore representation that catchment-
30 weathering DSi sources had, over the duration of MIS 5e. Changes to DSi supply are therefore

31 attributed to variations in within-lake conditions (e.g. turbulent mixing) over the period, where periods
32 of both high productivity and modelled-DSi supply (e.g. strong convective mixing) account for the
33 decreasing trend in $\delta^{30}\text{Si}_{\text{diatom}}$ compositions (after c. 124 ka BP).

34

35 **Key words**

36 Eemian, Kazantsevo, diatoms, silicon isotopes, Siberia, palaeoproductivity

37

38 **1. Introduction:**

39 Primary productivity is a key ecosystem function synthesizing organic matter. In deep lakes production
40 is usually dominated by phytoplankton. Over long timescales, primary production is controlled by a
41 number of external and internal drivers such as climate change, landscape evolution and lake ontogeny.
42 Species composition also has an important influence on productivity-diversity relationships (e.g.
43 Dodson et al., 2000). On Quaternary timescales palaeoproductivity may be estimated using a number of
44 different techniques, including palaeoecological (e.g. diatom analysis) biogeochemical (e.g. biogenic
45 silica or pigment analysis) or stable isotope approaches. Palaeoproductivity records allow us to test key
46 hypotheses related to climate variability, including differences between interglacial periods, which may
47 act as analogues to a future warming world. One of the most studied interglacials is the Last
48 Interglacial, a possible analogue for a future, warmer Earth (although in terms of orbital configuration,
49 this comparison is imperfect).

50

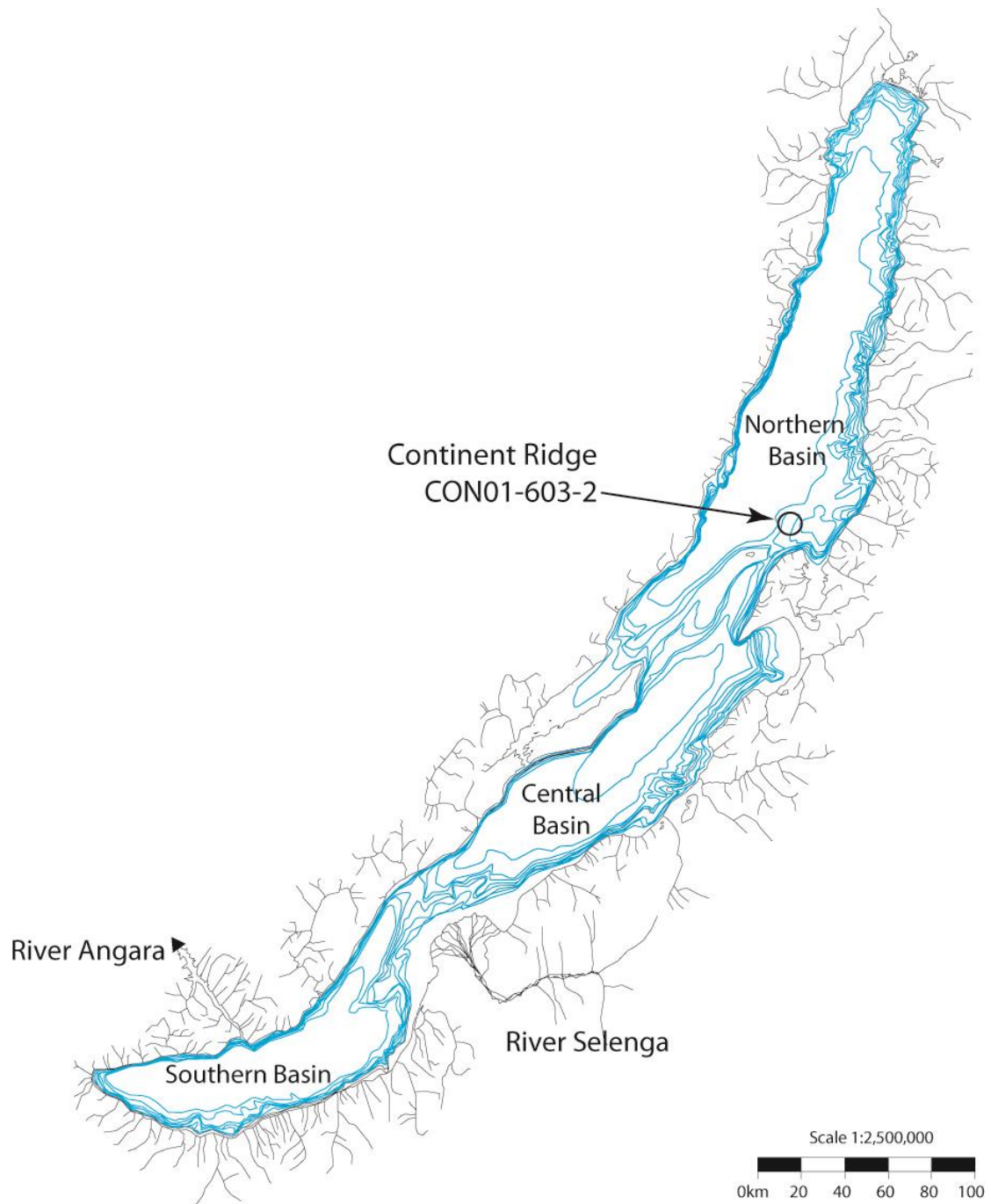
51 The Last Interglacial, corresponding to Marine Isotope Stage (MIS) 5e (130 - 115 ka BP; PAGES,
52 2016; Railsback et al., 2015), is often referred to as the Eemian in Western European continental
53 records, or in Siberia, the Kazantsevo. In order to more fully understand the nature, duration and
54 synchronicity of MIS 5e across the globe, the comparison of independent continental and oceanic
55 climate records are needed. Lake Baikal, Siberia (103°43'-109°58'E and 51°28'-55°47'N; Figure 1)
56 provides a key uninterrupted, continental sedimentary archive, which spans at least the past 20 million
57 years (Williams et al., 2001), to which further Eurasian continental records (e.g. loess sequences) can
58 be compared (Prokopenko et al., 2006). Lake Baikal is the world's deepest and most voluminous lake
59 (23, 615 km²) with a catchment of over 540, 000 km². Its mid-latitude location in central Asia means
60 that the lake is highly continental (Lydolph, 1977), and sensitive to obliquity- and precessional-driven

61 forcing (Short et al., 1991), which has allowed an astronomically tuned climate record for the entire
62 Pleistocene (Prokopenko et al., 2006).

63

64 **Figure 1.**

65 Map of Lake Baikal and its catchment with core CON-01-603-2 drilling location identified.



66

67

68

69 Prokopenko et al. (2001) argued that biogenic silica (BSi) records from Lake Baikal register regional
70 climatic fluctuations (e.g. glacial-interglacial cycles) and are linked to incoming solar radiation
71 (hereafter insolation) forcing, via heat balance exchanges within the lake (e.g. Prokopenko et al., 2006;
72 Prokopenko et al., 2001). At sub-orbital frequencies, BSi concentration may be related to regional
73 climate change, linked to teleconnections with shifting Atlantic Meridional Overturning Circulation
74 (e.g. Karabanov et al., 2000). On orbital timescales, Lake Baikal BSi records are interpreted as a
75 palaeoproductivity proxy (Mackay, 2007; Prokopenko et al., 2006; Prokopenko et al., 2001). Seasonal
76 phytoplankton succession at Lake Baikal today is influenced by the timing of ice-off (end of May-June)
77 and ice-on (after October), which promote a period of rapid diatom growth via upper water column
78 turbulent mixing (Popovskaya, 2000). The thermal regime of Lake Baikal in spring and autumn periods
79 is therefore very important in regulating diatom bloom development, together with the availability of
80 dissolved silicon (DSi) (Panizzo et al., in review; Popovskaya et al., 2015). While these productivity
81 proxies (e.g. BSi, in tandem with diatom assemblages) can provide an insight into variations in
82 limnological characteristics (e.g. length of growing season, lake turnover) over previous glacial-
83 interglacial cycles, they do not provide the ability to quantitatively assess variations between within-
84 lake, versus catchment, delivery of nutrients (namely DSi). We aim to address this in this study, via the
85 use of silicon stable isotope geochemistry to reconstruct such changes over the Last Interglacial.

86

87 There are three stable isotopes of silicon (Si: ^{28}Si , ^{29}Si and ^{30}Si), which fractionate during almost all
88 low-temperature processes of the continental and oceanic silicon cycles, highlighting their value as a
89 geochemical tracer. Variations in the isotope abundances (e.g. $^{30}\text{Si}/^{28}\text{Si}$ [although previously more
90 commonly $^{29}\text{Si}/^{28}\text{Si}$]) are reported via the delta notation ($\delta^{30}\text{Si}$), when compared to a known standard
91 reference material (e.g. NBS 28). Records of $\delta^{30}\text{Si}$ composition of waters and diatom opal ($\delta^{30}\text{Si}_{\text{DSi}}$ and
92 $\delta^{30}\text{Si}_{\text{diatom}}$ respectively) from Lake Baikal have demonstrated the clear relationship between diatom
93 biomass and nutrient availability (Panizzo et al., in review; Panizzo et al., 2017; Panizzo et al., 2016),
94 pointing to $\delta^{30}\text{Si}_{\text{diatom}}$ as a proxy for surface water DSi utilisation. This is because DSi (in the form of
95 silicic acid $[\text{Si}(\text{OH})_4]$) is a key nutrient for diatom uptake and growth (Martin-Jezequel et al., 2000).
96 During biomineralisation diatoms discriminate against the heavier isotopes (^{29}Si and ^{30}Si) over the
97 lighter (^{28}Si), which leads to the preferential isotopic enrichment of the residual solution (in this case,
98 the dissolved phase: $\delta^{30}\text{Si}_{\text{DSi}}$) in the heavier isotopes. This in turn leaves a clear biological imprint on

99 the isotopic composition of BSi (De La Rocha et al., 1997). The per mille fractionation or enrichment
100 factor (termed $^{30}\epsilon_{\text{uptake}}$) between both phases is considered to be between c. -1.1 and -1.6% (estimated
101 from freshwater systems; Alleman et al., 2005; Opfergelt et al., 2011; Panizzo et al., 2016; Sun et al.,
102 2013) and be independent of temperature, $p\text{CO}_2$ and nutrient availability (De La Rocha et al., 1997;
103 Fripiat et al., 2011; Milligan et al., 2004; Varela et al., 2004) some *in-vitro* studies on oceanic diatoms
104 have suggested a species dependent $^{30}\epsilon_{\text{uptake}}$ effect (Sutton et al., 2013). While this final attestation
105 remains in dispute, in the case of Lake Baikal *in-situ* estimations of diatom $^{30}\epsilon_{\text{uptake}}$ are c. -1.6% ,
106 derived from calculations of seasonal BSi (Panizzo et al., 2016). A final important consideration is the
107 preservation of the $\delta^{30}\text{Si}_{\text{diatom}}$ in surface sediments, where it is estimated that only c. 1% of total diatom
108 valves are preserved in Lake Baikal (Ryves et al., 2003). Despite this being a pervasive issue at this
109 site, Panizzo et al. (2016) demonstrate the absence of any diatom dissolution associated $^{30}\epsilon$ (as per
110 earlier studies by Demarest et al., 2009) and therefore validate the application of $\delta^{30}\text{Si}_{\text{diatom}}$
111 reconstructions from lake sediments.

112

113 On the basis of the above discussion and earlier work at Lake Baikal (Panizzo et al., In review; Panizzo
114 et al., 2017; Panizzo et al., 2016), we propose that $\delta^{30}\text{Si}_{\text{diatom}}$ sedimentary records can act as a tracer of
115 past diatom nutrient uptake. In addition, we apply silicon isotope geochemistry from Lake Baikal
116 sediments as a means to explore, in more detail, the catchment and within-lake constraints on silicon
117 cycling (via the application of independent diatom productivity proxies), as a means to understand how
118 climate has impacted nutrient supply, productivity and export at Lake Baikal over MIS 5e. Our
119 objectives are to provide, firstly, an overview of $\delta^{30}\text{Si}_{\text{diatom}}$ signatures in MIS 5e and determine if
120 diatom utilisation was higher than the current interglacial. Secondly, to reconstruct palaeo-nutrient
121 supply of DSi in Lake Baikal surface waters over the course of the Last Interglacial. In particular, we
122 compare these parameters with existing palaeolimnological proxies the better to reconstruct variations in
123 nutrient availability and diatom uptake, as a response to prevailing orbital and climatological changes.
124 Finally we devise a new interpretive model to best describe intra-Last Interglacial variability at Lake
125 Baikal.

126

127 **2. Materials and methods:**

128 **2.1. Core collection**

129 Core CON-01-603-2 was collected on the Continent Ridge, north basin, of Lake Baikal in July 2001 at
130 the location of 53°57' N, 108°54' E (Figure 1). The core was collected from a water depth of 386 m
131 using a piston corer, with full details provided by Demory et al. (2005a); Demory et al. (2005b) Charlet
132 et al. (2005). Detailed summaries on CON-01-603-2 core collection and chronology (radiocarbon and
133 palaeomagnetism) can be found therein. Sample resolution represents c. 200 years for the majority of
134 the record, although this increases to c. 400 years between 118 ka to 116 ka BP.

135

136 Here we present the methods for this new data set of $\delta^{30}\text{Si}_{\text{diatom}}$ alone, although reference is also made
137 to existing datasets of $\delta^{18}\text{O}_{\text{diatom}}$ (Mackay et al., 2013), diatom biovolume accumulation rates (BVAR)
138 (Rioual and Mackay, 2005), catchment weathering indices (e.g. sediment clay mineralogy; Fagel and
139 Mackay, 2008) and pollen-derived vegetation biome reconstructions (Tarasov et al., 2005; derived
140 from the pollen reconstructions of Granoszewski et al., 2005) from the same core (Figures 3,4).

141

142 **2.2. Silicon isotope preparation and analysis**

143 A total of 16 samples for $\delta^{30}\text{Si}_{\text{diatom}}$ analyses were selected across an existing $\delta^{18}\text{O}_{\text{diatom}}$ record (Mackay
144 et al., 2013) from sediment core CON-01-603-2. Samples underwent preparation to remove high
145 episodes of contamination (namely Al_2O_3) via more vigorous cleaning (of the existing diatom opal
146 from Mackay et al., 2013), including heavy density separation and organic material oxidation (as per
147 methods outlined in Morley et al., 2004). Prior to isotopic analysis, all samples were visually inspected
148 via a Zeiss Axiovert 40 C inverted microscope, while X-ray fluorescence (XRF) analyses were also
149 conducted in order to verify, quantitatively, their purity. All samples demonstrated no visual
150 contamination (e.g. clay) and quantitative estimations via XRF are <1% (with sample $\text{Al}_2\text{O}_3/\text{SiO}_2$
151 <0.01).

152

153 Alkaline fusion (NaOH) of cleaned diatom opal and subsequent ion-chromatography (via cation
154 exchange methods; BioRad AG50W-X12) followed methodologies outlined by Georg et al. (2006),
155 with further analytical and methodological practices mentioned in Panizzo et al. (2016). Samples were
156 analysed in wet-plasma mode using the high mass-resolution capability of a ThermoScientific Neptune
157 Plus MC-ICP-MS (multi collector inductively coupled plasma mass spectrometer) at the British
158 Geological Survey. A minimum of two analytical replicates were made per sample. Full analytical

159 methods are detailed in Panizzo et al. (2017; 2016), including practices applied to minimize instrument
160 induced mass bias and drift (e.g. Cardinal et al., 2003; Hughes et al., 2011). Full procedural blank
161 compositions from MC-ICP-MS analyses were 31 ng compared to typical fusion amounts of 3390 ng
162 and differed from sample compositions by < 0.5%. Using the worst-case scenario (i.e. calculated using
163 the sample with the lowest Si concentration) this level of blank could result in a potential shift in
164 sample composition by < 0.04%. All blank measurements therefore demonstrated an insignificant
165 effect relative to the typical <0.11‰ propagated sample uncertainties (Table 1) and no correction for
166 procedural blank was made.

167

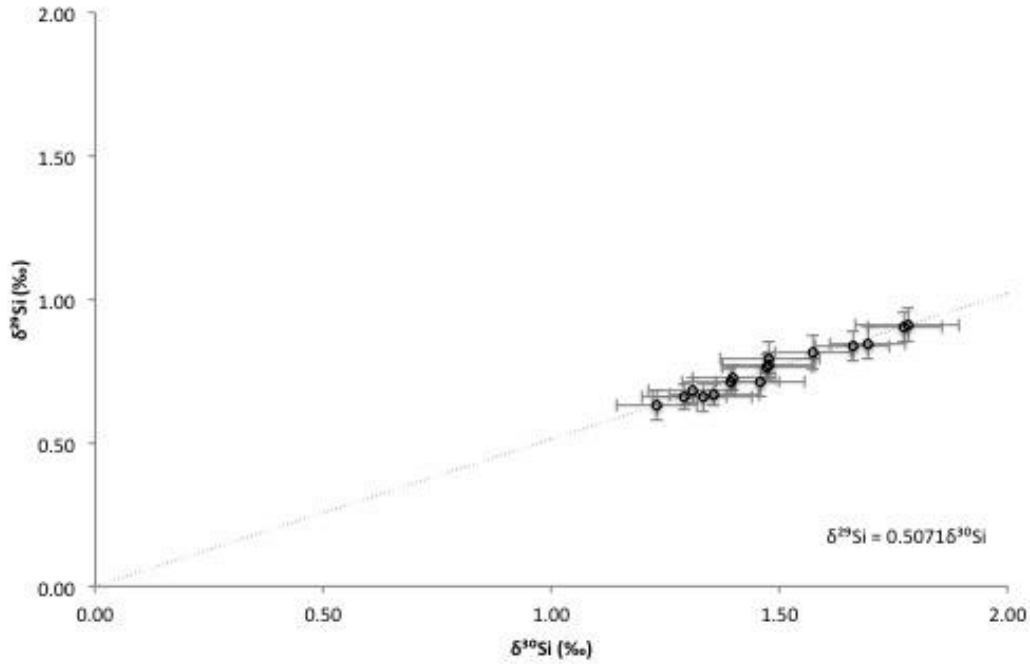
168 All uncertainties are reported at 2 sigma absolute (Table 1), and incorporate an excess variance derived
169 from the NBS 28 reference material, which was quadratically added to the analytical uncertainty of
170 each measurement. $\delta^{29}\text{Si}$ and $\delta^{30}\text{Si}$ were compared to the mass dependent fractionation line to which all
171 samples comply (Figure 2). Long term (~ 2 years) reproducibility and machine accuracy are assessed
172 via analyzing the Diatomite secondary standard and data agree with the published values: Diatomite =
173 $+1.24\text{‰} \pm 0.18\text{‰}$ (2 SD, n=244) (consensus value of $+1.26\text{‰} \pm 0.2\text{‰}$, 2 SD; Reynolds et al., 2007).

174

175 **Figure 2.**

176 Three-isotope plot ($\delta^{29}\text{Si}$ vs $\delta^{30}\text{Si}$) for all silicon isotope data (n=16) presented in this manuscript, with
177 data falling within analytical uncertainty of the mass-dependent fractionation line (dashed); in good
178 agreement with the kinetic fractionation of Si of 0.5092 (Reynolds et al., 2007).

179



180

181

182

183 2.3. Modelling palaeo-surface water nutrient availability

184 Based on an open system model approach (Eq. 1), which is considered most appropriate at Lake Baikal

185 (Panizzo et al., 2017), the equation can be re-arranged to calculate palaeo %DSi_{utilisation} (Eq. 2):

186

$$187 \quad \delta^{30}\text{Si}_{\text{DSi}} = \delta^{30}\text{Si}_{\text{initial}} - \epsilon_{\text{uptake}} (1 - f_{\text{Si}}) \quad \text{Eq. 1}$$

$$188 \quad \% \text{DSi}_{\text{utilisation}} = 1 - [(\delta^{30}\text{Si}_{\text{diatom}} - \delta^{30}\text{Si}_{\text{initial}}) / -\epsilon_{\text{uptake}}] \quad \text{Eq. 2}$$

189

190 Where $\delta^{30}\text{Si}_{\text{initial}}$ is the initial composition of the dissolved pool, before biological enrichment. We argue

191 that this acts as baseline surface water compositions when ice-off and turbulent mixing occurs, leading

192 to the first (larger) spring diatom bloom (Panizzo et al., 2017). Modern day deep water (>500m)

193 compositions from Lake Baikal vary between +1.71‰ and +1.77‰ (data derived from the south and

194 north basins respectively) (Panizzo et al., 2017). Taking into consideration a 2SD on these values

195 (0.04‰ and 0.03‰ respectively), a maximum and minimum likelihood $\delta^{30}\text{Si}_{\text{initial}}$ composition can be

196 calculated and a 95% confidence interval applied to modelled DSi utilization (Figures 3; 4). The

197 assumption that modern day $\delta^{30}\text{Si}_{\text{initial}}$ can be applied here may lead to some uncertainty in %DSi_{utilisation}

198 estimations (e.g. >100%; Table 1) however, in the absence of palaeo- $\delta^{30}\text{Si}_{\text{initial}}$ compositions from Lake

199 Baikal we argue its application here. $\delta^{30}\text{Si}_{\text{diatom}}$ is the isotopic composition of diatom opal at any given
200 time interval and $^{30}\epsilon_{\text{uptake}}$ is set at -1.6‰ , as discussed in Section 1 (Panizzo et al., 2017; Panizzo et al.,
201 2016).

202

203 In addition to simply quantifying past DSi surface utilisation via diatom biomineralisation, here we aim
204 to reconstruct palaeo-nutrient supply in Lake Baikal. As independent diatom productivity indicators
205 (e.g. BVAR) are also available from core CON-01-603-2, (Rioual and Mackay, 2005), an estimate of
206 DSi supply can be made by constraining $\delta^{30}\text{Si}_{\text{diatom}}$ compositions by the net export of BSi to sediments
207 (e.g. as a function of export production or nutrient demand; Horn et al., 2011). This application has
208 been seen in oceanic settings as a method to constrain better, reconstructions of nutrient supply, when
209 coupled with other algal productivity indicators (Horn et al., 2011).

210

$$211 \quad \text{DSi Supply} = \frac{F_{\text{BVAR}}^{\text{sample}} / F_{\text{BVAR}}^{120.5 \text{ ka}}}{\% \text{DSi}_{\text{consumed}}^{\text{sample}} / \% \text{DSi}_{\text{consumed}}^{120.5 \text{ ka}}} \quad \text{Eq. 3}$$

212

213 $F_{\text{BVAR}}^{\text{sample}}$ is the flux of BVAR in sediments and $\% \text{DSi}_{\text{consumed}}^{\text{sample}}$ is the percentage of the DSi consumed
214 by diatoms (in the sediment record). $F_{\text{BVAR}}^{120.5 \text{ ka}}$ and $\% \text{DSi}_{\text{consumed}}^{120.5 \text{ ka}}$ are defined as the sample with the
215 greatest modelled supply in the MIS 5e record (at c. 120.5 ka BP; Table 1). We apply the use of BVAR
216 here (over %BSi) as we argue this reflects more realistically the DSi demand of diatoms. Diatom
217 BVAR take into consideration diatom size (e.g. volume) and cell concentration, and so the amount of
218 DSi biomineralised in the valve (refer to Rioual and Mackay, 2005, for full explanation of calculation).
219 Diatom dissolution (defined as the percentage of pristine valves, of those preserved within the Lake
220 Baikal record; Rioual and Mackay, 2005; Table 1) across the MIS 6 to MIS 5d record is also
221 consistently $<23\%$, which supports the application of the proxy for modelling palaeo-DSi supply; i.e.
222 ruling out that dominant BVAR changes over this time over this record are a function of diatom
223 dissolution. BSi records on the other hand represent bulk biogenic opal in sediments, which has evaded
224 remineralisation (e.g. Ryves et al., 2003) and may not be exclusively diatomaceous in origin (e.g.
225 catchment derived amorphous silica). Zonation of Figure 4 and the discussion surrounding the
226 conceptual model at Lake Baikal (Section 4.2; Figure 5) is based on the Diatom Assemblage Zonations
227 (DAZ) defined by Rioual and Mackay (2005).

228

229 **3. Results:**

230 The data set presented here starts at the end of Termination 2 (c. 132 ka BP, n=1) through to the
231 transition from MIS 5e to MIS 5d at c. 116 ka BP. The resolution of sampling is at the millennial-scale,
232 c. every 850 years. All $\delta^{30}\text{Si}_{\text{diatom}}$ data range between +1.23 and +1.78‰ (0.17‰ 1SD of all final data,
233 n=16; Table 1). Lowest $\delta^{30}\text{Si}_{\text{diatom}}$ compositions are seen at c. 132.1 ka BP ($+1.23 \pm 0.09\text{‰}$, n=1; Table
234 1), during zone MIS 6. Highest values (between $+1.77 \pm 0.08\text{‰}$ and $+1.48 \pm 0.11\text{‰}$, n=7; Table 1) are
235 demonstrated in early MIS 5e (c. 127.4 and 123.0 ka BP), with a progression to lower values (c. $1.47 \pm$
236 0.1‰ and $+1.30 \pm 0.10$, n=8; Table 1) between c. 122.0 and 116.1 ka BP (Figure 3). There is one
237 episode of lower signatures, outside of the general MIS 5e decreasing trend, between c. 127.4 and
238 126.8 ka BP, where values fall to $+1.46 \pm 0.1\text{‰}$ (at c. 126.8 ka BP).

239

240 The linear approximation (via open system/steady state modelling) of DSi supply is portrayed in Table
241 1 and Figure 4. Percentage results are relative to the sample that has the highest modelled supply in the
242 record (e.g. 100% at c. 120.5 ka BP; Table 1). Results show an average c. 70% supply (range between
243 c. 64 and c. 100% over the period of MIS 5e) (e.g. c. 30% less supply than at 120.5 ka BP) after the
244 termination of the previous glacial MIS 6 (Figure 4). There is a step increase in modelled supply during
245 MIS 5e, after c. 124.9 ka, which is coincident with the continued decreasing trend in $\delta^{30}\text{Si}_{\text{diatom}}$
246 signatures and estimated %DSi utilisation over the course of the Last Interglacial (Figure 4).

247

248

249

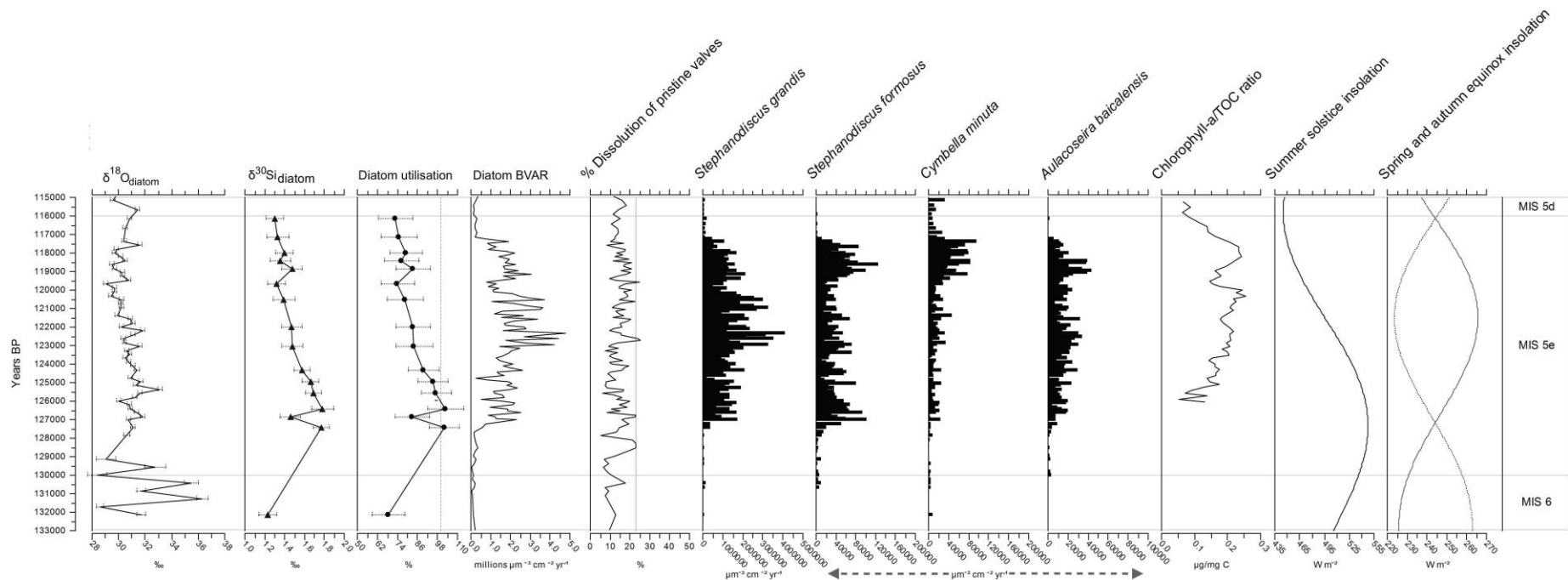
250 **Table 1**

251 $\delta^{30}\text{Si}_{\text{diatom}}$ and $\delta^{29}\text{Si}_{\text{diatom}}$ data (n=16) reported for the period 132.15 ka BP and 116.16 ka BP, with respective 2 sigma absolute analytical errors (‰). Sample names are
 252 provided in tandem with the modelled respective ages (ka BP) and mid-sediment sampling depth (CON-01-603-2). Data are presented with published total biovolume
 253 (millions $\mu\text{m}^{-3} \text{cm}^{-2} \text{year}^{-1}$) and % diatom dissolution index (Rioual and Mackay, 2005) data. The modelled open system %DSi utilisation and %DSi Supply (including
 254 maximum and minimum modelled likelihood errors) for each sample are also given.

| Sample Name | Mid-sediment depth (cm) | Dating profile (ka BP) | $\delta^{30}\text{Si}_{\text{diatom}}$ (‰) | ± 2 sigma absolute (‰) | $\delta^{29}\text{Si}_{\text{diatom}}$ (‰) | ± 2 sigma absolute (‰) | Biovolume (millions $\mu\text{m}^{-3} \text{cm}^{-2} \text{year}^{-1}$) | % Valve dissolution index | Modelled DSi Utilisation (%) | \pm Likelihood error (%) | Modelled DSi Supply (%) | \pm Likelihood error (%) |
|-------------|-------------------------|------------------------|--|----------------------------|--|----------------------------|--|---------------------------|------------------------------|----------------------------|-------------------------|----------------------------|
| EEM_12 | 613 | 116.16 | +1.29 | 0.09 | +0.66 | 0.04 | 0.27 | 15 | 73 | 11 | 9 | 1 |
| EEM_14 | 617 | 117.17 | +1.33 | 0.11 | +0.66 | 0.05 | 0.18 | 13 | 75 | 11 | 6 | 1 |
| EEM_18 | 625 | 118.00 | +1.40 | 0.09 | +0.73 | 0.04 | 1.81 | 13 | 79 | 10 | 59 | 8 |
| EEM_20 | 629 | 118.42 | +1.36 | 0.10 | +0.67 | 0.04 | 1.51 | 12 | 76 | 11 | 50 | 8 |
| EEM_22 | 633 | 118.84 | +1.47 | 0.10 | +0.77 | 0.05 | 1.39 | 21 | 83 | 11 | 43 | 6 |
| EEM_26 | 641 | 119.68 | +1.31 | 0.09 | +0.68 | 0.05 | 1.05 | 18 | 74 | 11 | 36 | 6 |
| EEM_30 | 649 | 120.53 | +1.39 | 0.11 | +0.72 | 0.04 | 3.06 | 15 | 78 | 11 | 100 | 16 |
| EEM_37 | 663 | 122.00 | +1.47 | 0.10 | +0.76 | 0.05 | 2.21 | 16 | 83 | 11 | 68 | 9 |
| EEM_42 | 673 | 123.05 | +1.48 | 0.11 | +0.80 | 0.06 | 1.23 | 9 | 84 | 11 | 38 | 5 |
| EEM_48 | 685 | 124.32 | +1.57 | 0.08 | +0.81 | 0.06 | 2.12 | 16 | 90 | 9 | 61 | 7 |
| EEM_51 | 691 | 124.95 | +1.66 | 0.08 | +0.84 | 0.05 | 1.56 | 8 | 95 | 9 | 42 | 4 |
| EEM_54 | 697 | 125.58 | +1.69 | 0.08 | +0.85 | 0.06 | 1.01 | 6 | 97 | 9 | 27 | 3 |
| EEM_58 | 705 | 126.42 | +1.78 | 0.11 | +0.91 | 0.06 | 1.55 | 10 | 102 | 11 | 39 | 4 |
| EEM_60 | 709 | 126.85 | +1.46 | 0.10 | +0.72 | 0.05 | 1.02 | 23 | 82 | 11 | 32 | 4 |
| EEM_62 | 713 | 127.44 | +1.77 | 0.08 | +0.90 | 0.05 | 0.47 | 15 | 102 | 9 | 12 | 1 |
| EEM_73 | 735 | 132.15 | +1.23 | 0.09 | +0.63 | 0.05 | 0.11 | 13 | 68 | 10 | 4 | 1 |

255

256



257

258

259

Figure 3.

260

Stratigraphic plot displaying $\delta^{18}\text{O}_{\text{diatom}}$ (‰) from Mackay et al. (2013) (note that data before c. 128 ka BP are not plotted due to contamination issues outlined by the authors),

261

$\delta^{30}\text{Si}_{\text{diatom}}$ (‰) with respective analytical errors, modelled %DSi utilisation (95% confidence intervals shown) from this dataset (open system model), total diatom biovolume

262

accumulation rates (BVAR) (millions $\mu\text{m}^{-3}\text{cm}^{-2}\text{year}^{-1}$) (Rioual and Mackay, 2005), % valve dissolution index (defined as the percentage of pristine valves, of those

263

preserved within in the record; Table 1) (Rioual and Mackay, 2005), dominant diatom species BVAR (thousands/millions $\mu\text{m}^{-3}\text{cm}^{-2}\text{year}^{-1}$) (Rioual and Mackay, 2005),

264

Chlorophyll a/TOC data ($\mu\text{g}/\text{mg C}$; Fietz et al., 2007) and insolation at 55°N (W m^{-2}) for the summer solstice and winter, spring (dashed) equinoxes. All sediment core

265

proxies presented are derived from core CON-01-603-2 (Figure 1).

266

267 4. Discussion

268 4.1. $\delta^{30}\text{Si}_{\text{diatom}}$ signatures during MIS 5e

269 The main focus of this discussion spans the MIS 5e period, although one data point of the record is
270 derived from the MIS 6 glacial (before c. 130 ka BP; Table 1, Figure 3). The ranges of values presented
271 here (from sediments collected from the North Basin; Figure 1) ($+1.23$ to $+1.78 \pm 0.17\%$; Table 1)
272 encompass mean modern day south basin surface sediment $\delta^{30}\text{Si}_{\text{diatom}}$ signatures ($+1.23\% \pm 0.08$ 1 SD;
273 Panizzo et al., 2016), especially the MIS 6 value. The $\delta^{30}\text{Si}_{\text{diatom}}$ data presented over MIS 5e (in
274 particular c. 127.4 ka BP to c. 116 ka BP) displays an overall decreasing trend concomitant, and
275 significantly correlated with, the decrease in June (solstice) insolation (at 55°N) ($r^2=0.53$, $p=0.001$).
276 However, there is an absence of correlation between $\delta^{30}\text{Si}_{\text{diatom}}$ and insolation (at 55°N) records of each
277 spring and autumn equinoxes (Figure 3) or winter solstice (data not shown). Furthermore, Last
278 Interglacial $\delta^{30}\text{Si}_{\text{diatom}}$ values (between $+1.30 \pm 0.10\%$ and $+1.77 \pm 0.08\%$; Table 1) are significantly
279 higher than Holocene $\delta^{30}\text{Si}_{\text{diatom}}$ compositions (Panizzo et al, unpublished data) derived from sediment
280 cores across all three Lake Baikal basins ($p=0.001$, via a Kruskal Wallis test).

281

282 Palaeoecological records in the Lake Baikal suggest that the climate was warmer and wetter during the
283 Last Interglacial than the Holocene (Tarasov et al., 2007), which in turn may account for the higher
284 $\delta^{30}\text{Si}_{\text{diatom}}$ -inferred utilisation over this period (Figure 3). Given the significantly higher $\delta^{30}\text{Si}_{\text{diatom}}$
285 signatures for MIS 5e we can interpret this as a period of either higher utilisation of DSi by diatoms
286 (e.g. enhanced productivity) and/or a weakened supply of nutrients to the surface (e.g. reduced
287 convective mixing or catchment derived nutrients). These arguments will be discussed further in the
288 following section, in conjunction with other climate and productivity indicators from Lake Baikal
289 during MIS 5e.

290

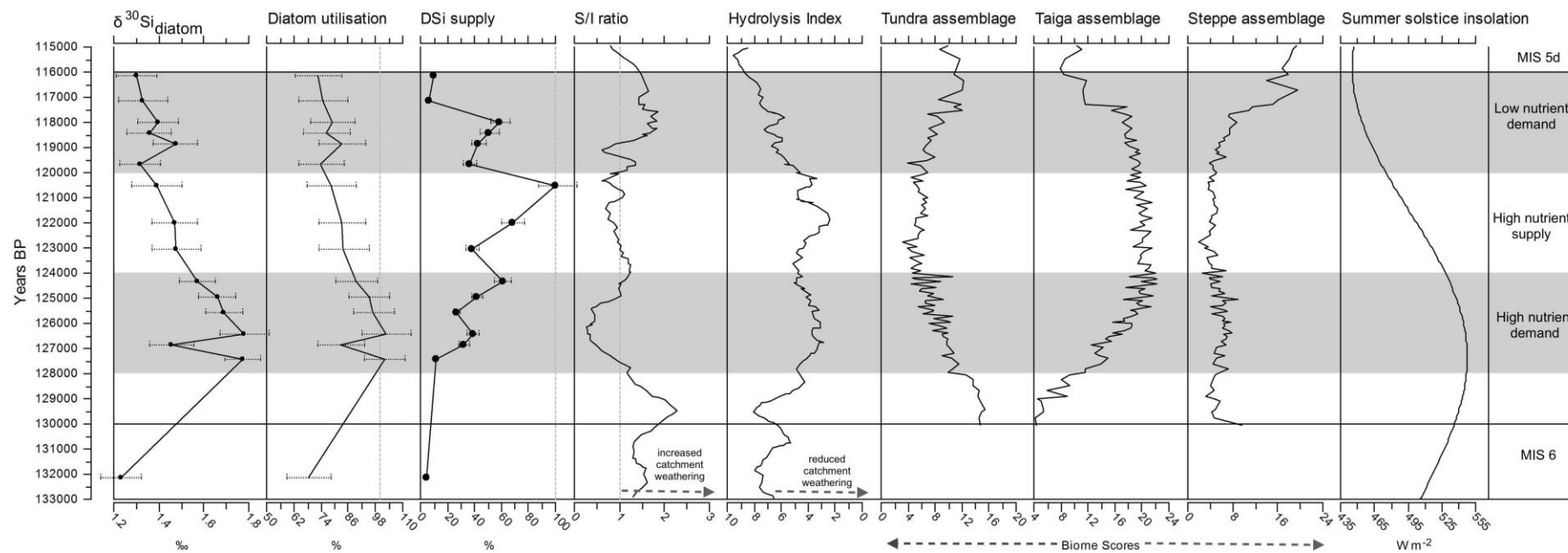
291

292

293
294
295
296
297
298

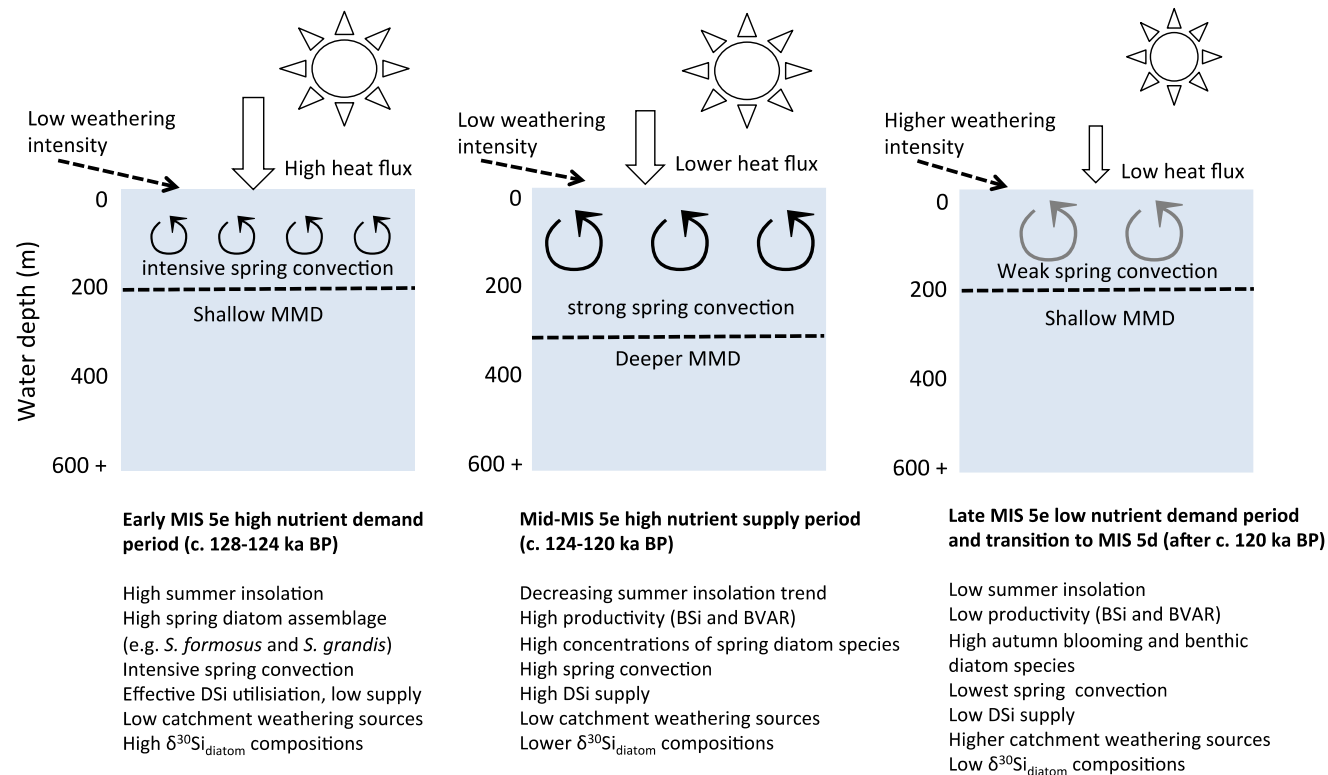
Figure 4.

Summary diagram of $\delta^{30}\text{Si}_{\text{diatom}}$ (‰) with respective analytical errors, modelled %DSi utilisation and estimated %DSi supply (with 95% confidence intervals), both constrained by BVAR. S/I ratios and the Hydrolysis Index (note reverse axis) (Fagel et al., 2005), along with dominant catchment biome scores (Tarasov et al., 2005) and summer solstice insolation at 55°N (W m^{-2}) are also displayed. Lines correspond to the time transition from MIS 6 to MIS 5e and MIS 5d. Shaded areas correspond to the interpretation of lake nutrient cycling as described in Section 4.2 and Figure 5 (defined as the DAZ of Rioual and Mackay, 2005).



299
300
301
302

303 **Figure 5.** A schematic nutrient-productivity model for the Lake Baikal upper water column (including surface waters to the MMD), during the Last Interglacial. Three
 304 interpretive periods are identified (Section 4.2) for MIS 5e and a description of the dominant drivers of upper water column nutrient availability (e.g. catchment versus
 305 within-lake) are provided. A summary of the dominant palaeoecological characteristics of these periods is also provided (based on Figures 3, 4), along with the main climatic
 306 forcing (e.g. insolation).
 307



308 **4.2. A conceptual model of diatom responses to altering DSi supply during the Last Interglacial**

309 A hydrodynamic-insolation model for the Lake Baikal BSi signal was proposed by Prokopenko et al.
310 (2001), where two models were put forward for diatom productivity during either interglacial (high
311 insolation and high BSi) or glacial (low insolation and low BSi) stages. However, as intra-Last
312 Interglacial climate variability has been demonstrated (including cooling; Karabanov et al., 2000;
313 atmospheric circulation and hydrological regime changes in the catchment; Mackay et al., 2013; and
314 changes in primary productivity; Rioual and Mackay, 2005), we here propose a more sensitive
315 interpretation via the application of diatom BVAR (Section 2.3; Figure 5). This revised nutrient-
316 productivity model reflects the variation captured in both diatom utilisation and nutrient (DSi) supply
317 over the course of MIS 5e (Figure 4), which was otherwise not accounted for in earlier models (e.g.
318 Prokopenko et al, 2001).

319

320 For the purpose of this discussion, we consider the delivery of nutrients (DSi) from both within-lake
321 (upwelling) and catchment derived processes. The Hydrolysis Index (HI) (Figure 4) of Fagel and
322 Mackay (2008) can be used to examine catchment weathering in Lake Baikal as a function of climatic
323 conditions, parent rock type and catchment topography (Fagel and Boes, 2008). Higher values (>5)
324 therefore indicate a greater presence of secondary minerals (e.g. increased weathering), while lower
325 values are indicative of primary mineral clay sources in sediments (e.g. reduced catchment
326 weathering). Meanwhile, smectite/illite ratios (S/I) are indicative of increased chemical weathering
327 (>1) or increased physical catchment weathering (<1), with illite being defined as one parent mineral
328 endmember for the site (Fagel and Mackay, 2008). In terms of silicon geochemistry, chemical
329 weathering of silicate rocks and minerals are attributable to the DSi load of rivers and ultimately lakes
330 and oceans (e.g. Stumm and Wollast, 1990) however physical erosion, controlled by climate, soil
331 formation and catchment vegetation, can also play an important role in deriving continental DSi fluxes
332 (Gaillardet et al., 1999). Under low erosion rates, weathering is regarded to be supply-limited; so that
333 clay mineral formation is higher (than primary mineral dissolution), which will reduce DSi fluxes
334 (relative to parent material)(e.g. low $DSi/[Na+K]^*$; Fontorbe et al., 2013; Frings et al., 2015; Hughes et
335 al., 2013) and preferentially discriminate against the heavy isotopes (indicative of higher river $\delta^{30}Si_{DSi}$
336 signatures). This interpretation is referred to as incongruent weathering (refer to the comprehensive
337 discussion of Frings et al., 2016 and references therein). The opposite scenario (kinetic-limited or more

338 congruent weathering) occurs under higher physical erosion rates (e.g. low weathering intensity [W/D];
339 Bouchez et al., 2014), where the rapid removal of material and low riverine/sedimentary residence
340 times reduces the accumulation of secondary mineral phases (high $\text{DSi}/[\text{Na}+\text{K}]^*$, higher DSi fluxes and
341 lower river $\delta^{30}\text{Si}_{\text{DSi}}$ signatures).

342

343 Quantitative catchment reconstructions of palaeo-weathering fluxes and DSi inflow compositions to
344 Lake Baikal are limited here due to the absence of catchment or riverine endmembers (from MIS 5e).
345 The overall need to expand silicon isotope continental paleo-weathering reconstructions has been
346 highlighted by Frings et al. (2016), although the greatest interest to date centers on quantifying river
347 $\delta^{30}\text{Si}_{\text{DSi}}$ signature variation to oceans (e.g. continental export) over glacial-interglacial cycles. Given
348 that the global river $\delta^{30}\text{Si}_{\text{DSi}}$ signatures exported to the ocean, between glacial-interglacial cycles, are
349 modelled to be only small e.g. estimated globally to increase only c. $0.2 \pm 0.25\%$ since the Last Glacial
350 Maximum following a reduction in weathering congruency (Frings et al., 2016) it is probable that intra-
351 Eemian variability of weathering regimes also has a small impact on altering Lake Baikal source waters
352 over this time. However, we here use the HI and S/I ratio of Fagel and Mackay (2008) as an
353 independent palaeo-weathering proxy to explore this argument and constrain any catchment derived
354 sources of DSi for diatom biomineralisation.

355

356 Three descriptive zones (derived from the DAZ of Rioual and Mackay, 2005; shaded in Figure 4) are
357 applied to examine variations in $\delta^{30}\text{Si}_{\text{diatom}}$ over the Last Interglacial, as a response to regional climate
358 changes and insolation forcing (Figure 5). We propose that while catchment changes (e.g. biome shifts
359 and weathering rates) may have played a role in regulating catchment DSi supply into Lake Baikal
360 waters (via rivers) over the course of MIS 5e (Figure 4), these act as more mediated responses. Rather
361 we propose that, as today, within-lake processes (reduced lake ice duration and increased turbulent,
362 convective mixing) are more rapid responses to, and therefore act as, the dominant driver in controlling
363 surface waters nutrient change over this time. Below we present a palaeoecological interpretation of the
364 three descriptive zonations (for MIS 5e alone), to which we propose this new interpretation of diatom
365 and nutrient responses over this period (Figure 5).

366

367 *4.2.1. Early MIS 5e high nutrient demand period (c. 128-124 ka BP):*

368 The increase to higher $\delta^{30}\text{Si}_{\text{diatom}}$ signatures in MIS 5e (after c. 127.4 ka BP) occurs at peak summer
369 insolation and is also coincident with the increase in diatom BVAR (Rioual and Mackay, 2005) and
370 BSi records (derived from different composite cores from the Academician Ridge; Prokopenko et al.,
371 2006) and later (after c. 126 ka BP) Chlorophyll-*a* (Figure 3). Mackay et al. (2013) interpret $\delta^{18}\text{O}_{\text{diatom}}$
372 data to reflect a period of increased river discharge to Lake Baikal, in response to regional warming
373 (increased pollen-inferred precipitation and temperatures; Tarasov et al., 2007; Tarasov et al., 2005), a
374 weaker Siberian High (Velichko et al., 1991) and teleconnections with the North Atlantic (lowest
375 global ice volume; Kukla et al., 2002; and warmer North Atlantic sea surface temperatures; Oppo et al.,
376 2006). Apart from a brief reduction in $\delta^{30}\text{Si}_{\text{diatom}}$ signatures to +1.46‰ (± 0.10 2 sigma) at c. 126.8 ka
377 BP, values otherwise remain high during this period.

378

379 Both HI and S/I ratios are low after c. 128 ka BP (after a decreasing trend at the start of MIS 5e; Figure
380 4), which is indicative of physical (over chemical) weathering processes dominating in the catchment,
381 with limited secondary mineral formation in soils (e.g. low weathering intensity and higher proportion
382 of primary minerals in lake sediments) (Fagel and Mackay, 2008). During this period, these conditions
383 are concomitant with high summer insolation (Figures 4; 5) and an increase taiga biome scores,
384 indicative of a warming climate (Tarasov et al., 2007; Tarasov et al., 2005). Although the low S/I ratios
385 (the lowest in the record during this period) highlight changes in sediment clay mineralogy, which are a
386 result of soil destabilization in the catchment (Fagel and Mackay, 2008), the low HI is indicative of a
387 low weathering intensity regime (with probable low fractionation potential of river waters). This
388 interpretation compares well with BVAR-modelled DSi supply, which is among the lowest of the
389 whole record (40-90% less than peak supply at c. 120.5 ka BP; Table 1). Taken together these data
390 suggest that the magnitude of change to catchment DSi source waters was not great enough to alter
391 considerably, pelagic source waters, so that the high $\delta^{30}\text{Si}_{\text{diatom}}$ signatures are driven more strongly by
392 diatom biomineralisation.

393

394 During the “high nutrient demand period” (c. 128 to 124 ka BP), spring blooming species
395 *Stephanodiscus formosus* and *Stephanodiscus grandis* (the latter which contributes the greatest to
396 diatom BVAR; Figure 3) also increase, along with other *Aulacoseira baicalensis* and *Aulacoseira*
397 *skvortzowii* species (Rioual and Mackay, 2005). Although these *Stephanodiscus* species are today

398 extinct, based on modern analogues, Rioual and Mackay (2005) attribute them to be slow growing due
399 to their large size, tolerant of low light conditions with a high phosphorus and moderate silica demand,
400 associated today with long deep convective spring mixing (up to 300 m; Shimaraev et al., 1993). These
401 data point to the interpretation of enhanced nutrient exchange in surface waters at the beginning of MIS
402 5e, and a productive initial spring diatom bloom, dominated by the high phosphorus, moderate DSi,
403 nutrient demand *Stephanodiscus* species (Figures 3,4). With low-modelled DSi supply over this period
404 (including from catchment sources), $\delta^{30}\text{Si}_{\text{diatom}}$ compositions become more enriched with an overall
405 switch to higher diatom productivity (BVAR; Figures 3, 4) and DSi utilisation, following MIS 6.

406

407 4.2.2. Mid-MIS 5e high nutrient supply period (c. 124-120 ka BP)

408 Estimated DSi utilisation is low after c. 124 ka BP, suggesting more nutrient rich conditions,
409 concomitant with the decreasing trend in $\delta^{30}\text{Si}_{\text{diatom}}$ signatures and step shift in higher diatom BVAR
410 (Figure 4). This trend also follows the decreasing summer insolation and $\delta^{18}\text{O}_{\text{diatom}}$ compositions
411 (Figures 3, 4), although the catchment is composed of a stable taiga biome (Figure 4; Tarasov et al.,
412 2007; Tarasov et al., 2005). Clay mineralogy (S/I ratio) during this zone continues to suggest
413 conditions indicative of physical (over chemical) weathering, with sediments dominated by primary
414 mineral sources (low HI; Figure 4) and therefore low chemical weathering in the catchment over this
415 period. We interpret the record therefore to point to a continued low weathering intensity (Section
416 4.2.1). As Lake Baikal catchment conditions appear relatively stable during this zone (based on pollen
417 and clay mineralogy) but modelled DSi supply increases (Figure 4), which we suggest is due to within-
418 lake DSi sources (e.g. increased mixing) being more important in driving lower $\delta^{30}\text{Si}_{\text{diatom}}$ signatures
419 (i.e. increased supply versus reduced diatom uptake) rather than an increased catchment derived source
420 of DSi (e.g. of lower $\delta^{30}\text{Si}_{\text{DSi}}$ composition).

421

422 Estimated supply increases during this period (c. 124 to 120 ka BP) reaching the time of highest
423 modelled supply (100%) at 120.5 ka BP (Table 1), concomitant with highest diatom BVAR and
424 increased Chlorophyll-*a* concentrations (Fietz et al., 2007) (Figure 3). The increase in diatom BVAR is
425 again attributed to the increase in *S. grandis* species (Rioual and Mackay, 2005), which proportionally
426 dominates diatom biovolumes over MIS 5e. We propose (based on modern-analogue diatom ecology)
427 a shift towards a deeper mesothermal maximum depth (MMD; Figure 5), concomitant with a deeper

428 spring mixing layer compared to the previous period. This will account for the increase in DSi supply
429 to surface waters and therefore some of the lowest $\delta^{30}\text{Si}_{\text{diatom}}$ compositions in the reconstruction, despite
430 increased diatom productivity.

431

432 4.2.3 Low nutrient demand period and the transition to MIS 5d (after 120 ka BP)

433 After c. 120.4 ka BP Rioual and Mackay (2005) document a notable change in individual diatom
434 species BVAR at Lake Baikal, from the large-celled *Stephanodiscus* species to smaller celled
435 *Cyclotella* species, especially *Cyclotella minuta* (Figures 3; 5). *C. minuta* can tolerate relatively high
436 summer surface water temperatures (e.g. during stratification), so that when autumnal mixing begins
437 they are among the first species to bloom (Jewson et al., 2015). These species changes are concomitant
438 with a stepwise decrease in total diatom BVAR, which points to a decrease in overall diatom
439 productivity in Lake Baikal (Figure 3). Decreasing $\delta^{30}\text{Si}_{\text{diatom}}$ compositions and modelled DSi utilisation
440 may further corroborate this reduction in productivity, leading to the interpretation of reduced DSi
441 demand (due to both reduced productivity and the prevalence of smaller diatom species) (Figure 5).
442 Overall we propose conditions less favorable for larger spring blooming species (e.g. *S. grandis*). In
443 particular, overall reduced productivity is attributed to weaker spring convective mixing, the
444 breakdown in thermal driven stratification and a reduction in the overall growing season (increased ice
445 cover duration) consistent with the move to cooler conditions in the region (Figure 5).

446

447 Superimposed on these trends is a minimum in $\delta^{18}\text{O}_{\text{diatom}}$ compositions between c. 120.5 and 119.7 ka
448 BP (Figure 3), which Mackay et al. (2013) attribute to a cold perturbation in the Lake Baikal region (an
449 increase in Siberian High intensity; Tarasov et al., 2005) with increased snowmelt contributions and a
450 reduction in primary productivity (Fietz et al., 2007; Prokopenko et al., 2006; Rioual and Mackay,
451 2005). Similarly, $\delta^{30}\text{Si}_{\text{diatom}}$ signatures also show a small (although within analytical uncertainty)
452 decline, which could be reflecting reduced diatom productivity during this cold event and therefore low
453 DSi uptake (and low modelled DSi supply) (Figures 4, 5). Interestingly, S/I ratios and HI increase after
454 c. 120 ka BP (Figure 4), which points to an increase in chemical weathering (intensity) in the Lake
455 Baikal catchment (e.g. towards supply-limited weathering regimes, indicative of higher river $\delta^{30}\text{Si}_{\text{DSi}}$),
456 although as there are no large changes in $\delta^{30}\text{Si}_{\text{diatom}}$ compositions after this time, we again suggest that

457 isotopically altered source waters to the lake have not had a confounding impact in driving $\delta^{30}\text{Si}_{\text{diatom}}$
458 signatures after this time.

459

460 After c. 117.2 ka BP benthic diatom species increase in relative abundance (Rioual and Mackay, 2005).
461 This, along with a sharp fall in diatom BVAR and Chlorophyll-*a* concentrations (Fietz et al., 2007),
462 points to a reduction in pelagic productivity indicative of a switch to a much colder climate after this
463 time, coincident with a continued decline in summer insolation, a shift to increased steppe biomes
464 scores (Figure 4) and reduced mean summer temperatures (Tarasov et al., 2007; Tarasov et al., 2005),
465 all while ice sheet growth occurred in the Northern Hemisphere (Kukla et al., 2002).

466

467 **5. Conclusions**

468 Here we present the first application of $\delta^{30}\text{Si}_{\text{diatom}}$ in the palaeorecord at Lake Baikal and present it as a
469 proxy for both nutrient availability and demand over the Last Interglacial (MIS 5e). Overall, diatom
470 productivity is significantly higher in MIS 5e compared to the Holocene. In tandem with other
471 published productivity indicators from core CON-01-603-2, data point to an early interglacial stage of
472 high DSi demand by diatoms, although low nutrient conditions, in response to regional climate
473 warming, catchment vegetation and weathering regime changes. After c. 124 ka BP data suggest a
474 move to higher nutrient supply, although we attribute this to an increase in spring convective mixing
475 based on overall reconstructions of a stable Lake Baikal catchment (e.g. weathering indices and
476 vegetation). We propose complex within-lake conditions over the duration of MIS 5e, based on the
477 variability in diatom nutrient uptake and surface water nutrient availability (e.g. driven by changes in
478 lake ice duration and turbulent convective mixing). Unlike the earlier interpretative palaeoproductivity
479 models based on BSi data alone, we derive a more nuanced reconstruction highlighting that more
480 caution should be taken to understand fully the mechanisms at play during both inter- and intra-
481 interglacial/glacial climates. This will better inform the sensitivity and response of Lake Baikal to
482 climate change both in the past and under future anthropogenic and climate pressures.

483

484

485 **Acknowledgements:**

486 This work was supported by the Natural Environmental Research Council [grant number
487 NE/J00829X/1]. AWM acknowledges contributions from the EU FPV Project “CONTINENT” (Ref:
488 EKV2-2000-00057), for funding previous Last Interglacial studies on Lake Baikal.

489 **References:**

- 490
- 491 Alleman, L.Y., Cardinal, D., Cocquyt, C., Plisnier, P.D., Descy, J.P., Kimirei, I., Sinyinza, D., André,
492 L., 2005. Silicon isotopic fractionation in Lake Tanganyika and its main tributaries. *J. Great Lakes Res.*
493 31, 509-519
- 494 Bouchez, J., Gaillardet, J., von Blackenburg, F., 2014. Weathering intensity in lowland river basins:
495 from the Andes to the Amazon mouth. *Procedia Earth Planetary Sciences* 10, 280-286
- 496 Cardinal, D., Alleman, L.Y., de Jong, J., Ziegler, K., André, L., 2003. Isotopic composition of silicon
497 measured by multicollector plasma source mass spectrometry in dry plasma mode. *J. Anal. At.*
498 *Spectrom.* 18, 213-218. doi: 10.1039/B210109b
- 499 Charlet, F., Fagel, N., De Batist, M., Hauregard, F., Minnebo, B., Meischner, D., SONIC Team., 2005.
500 Sedimentary dynamics on isolated highs in Lake Baikal: evidence from detailed high-resolution
501 geophysical data and sediment cores. *Global Planet. Change* 46, 125-144. doi:
502 10.1016/J.Gloplacha.2004.11.009
- 503 De La Rocha, C.L., Brzezinski, M.A., DeNiro, M.J., 1997. Fractionation of silicon isotopes by marine
504 diatoms during biogenic silica formation. *Geochim. Cosmochim. Acta* 61, 5051-5056. doi:
505 10.1016/s0016-7037(97)00300-1
- 506 Demarest, M.S., Brzezinski, M.A., Beucher, C.P., 2009. Fractionation of silicon isotopes during
507 biogenic silica dissolution. *Geochim. Cosmochim. Acta* 73, 5572-5583. doi:10.1016/j.gca.2009.06.019
- 508 Demory, F., Nowaczyk, N.R., Witt, A., Oberhansli, H., 2005a. High-resolution magneto stratigraphy of
509 late quaternary sediments from Lake Baikal, Siberia: timing of intracontinental paleoclimatic
510 responses. *Global Planet. Change* 46, 167-186. doi: 10.1016/j.gloplacha.2004.09.016
- 511 Demory, F., Oberhansli, H., Nowaczyk, N.R., Gottschalk, M., Wirth, R., Naumann, R., 2005b. Detrital
512 input and early diagenesis in sediments from Lake Baikal revealed by rock magnetism. *Global Planet.*
513 *Change* 46, 145-166. doi:10.1016/j.gloplacha.2004.11.010
- 514 Dodson, S.I., Arnott, S.W., Cottingham, K.L., 2000. The relationship in lake communities between
515 primary productivity and species richness. *Ecology* 81, 2662-2679
- 516 Fagel, N., Alleman, L.Y., Granina, L., Hatert, F., Thamo-Bozso, E., Cloots, R., André, L., 2005.
517 Vivianite formation and distribution in Lake Baikal sediments. *Global Planet. Change* 46, 315-336. doi:
518 10.1016/J.Gloplacha.2004.09.022
- 519 Fagel, N., Boes, X., 2008. Clay-mineral record in Lake Baikal sediments: The Holocene and Late
520 Glacial transition. *Palaeogeography Palaeoclimatology Palaeoecology* 259, 230-243.
521 doi:10.1016/j.palaeo.2007.10.009
- 522 Fagel, N., Mackay, A.W., 2008. Weathering in the Lake Baikal watershed during the Kazantsevo
523 (Eemian) interglacial: Evidence from the lacustrine clay record. *Palaeogeography Palaeoclimatology*
524 *Palaeoecology* 259, 244-257. doi: 10.1016/J.Palaeo.2007.10.011
- 525 Fietz, S., Nicklisch, A., Oberhansli, H., 2007. Phytoplankton response to climate changes in Lake
526 Baikal during the Holocene and Kazantsevo Interglacials assessed from sedimentary pigments. *J.*
527 *Paleolimnol.* 37, 177-203. doi: 10.1007/s10933-006-9012-y
- 528 Fontorbe, G., De La Rocha, C.L., Chapman, H.J., Bickle, M.J., 2013. The silicon isotopic composition
529 of the Ganges and its tributaries. *Earth. Planet. Sci. Lett.* 381, 21-30. doi: 10.1016/J.Epsl.2013.08.026
- 530 Frings, P.J., Clymans, W., Fontorbe, G., De La Rocha, C.L., Conley, D.J., 2016. The continental Si
531 cycle and its impact on the ocean Si isotope budget. *Chem. Geol.* 425, 12-36. doi:
532 10.1016/j.chemgeo.2016.01.020

- 533 Frings, P.J., Clymans, W., Fontorbe, G., Gray, W., Chakrapani, G.J., Conley, D.J., De La Rocha, C.,
534 2015. Silicate weathering in the Ganges alluvial plain. *Earth. Planet. Sci. Lett.* 427, 136-148.
535 doi:10.1016/j.epsl.2015.06.049
- 536 Fripiat, F., Cavagna, A.J., Dehairs, F., Speich, S., André, L., Cardinal, D., 2011. Silicon pool dynamics
537 and biogenic silica export in the Southern Ocean inferred from Si-isotopes. *Ocean Sci.* 7, 533-547.
538 doi:10.5194/os-7-533-2011
- 539 Gaillardet, J., Dupré, B., Louvat, P., Allègre, C.J., 1999. Global silicate and CO₂ consumption rates
540 deduced from the chemistry of large rivers. *Chem. Geol.* 159, 3-30
- 541 Georg, R.B., Reynolds, B.C., Frank, M., Halliday, A.N., 2006. New sample preparation techniques for
542 the determination of Si isotopic compositions using MC-ICP-MS. *Chem. Geol.* 235, 95-104. doi:
543 10.1016/J.Chemgeo.2006.06.006
- 544 Granoszewski, W., Demske, D., Nita, M., Heumann, G., Andreev, A., 2005. Vegetation and climatic
545 variability during the Last interglacial evidenced in the pollen record from Lake Baikal. *Global Planet.*
546 *Change* 46, 187-198
- 547 Horn, M.G., Beucher, C.P., Robinson, R.S., Brzezinski, M.A., 2011. Southern ocean nitrogen and
548 silicon dynamics during the last deglaciation. *Earth. Planet. Sci. Lett.* 310, 334-339. doi:
549 10.1016/j.epsl.2011.08.016
- 550 Hughes, H.J., Delvigne, C., Korntheuer, M., de Jong, J., André, L., Cardinal, D., 2011. Controlling the
551 mass bias introduced by anionic and organic matrices in silicon isotopic measurements by MC-ICP-
552 MS. *J. Anal. At. Spectrom.* 26, 1892-1896. doi: 10.1039/C1ja10110b
- 553 Hughes, H.J., Sondag, F., Santos, R.V., André, L., Cardinal, D., 2013. The riverine silicon isotope
554 composition of the Amazon Basin. *Geochim. Cosmochim. Acta* 121, 637-651. doi:
555 10.1016/j.gca.2013.07.040
- 556 Jewson, D.H., Granin, N.G., Gnatovsky, R.Y., Lowry, S.F., Teubner, K., 2015. Coexistence of two
557 *Cyclotella* diatom species in the plankton of Lake Baikal. *Freshwat. Biol.* 60, 2113-2126. doi:
558 10.1111/fwb.12636
- 559 Karabanov, E., Prokopenko, A.A., Williams, D., Khursevich, G., 2000. Evidence for mid-Eemian
560 cooling in continental climatic record from Lake Baikal. *J. Paleolimnol.* 23, 365-371
- 561 Kukla, G.J., Bender, M.L., de Beaulieu, J.L., Bond, G., Broecker, W.S., Cleveringa, P., Gavin, J.E.,
562 Herbert, T.D., Imbrie, J., Jouzel, J., Keigwin, L.D., Knudsen, K.L., McManus, J.F., Merkt, J., Muhs,
563 D.R., Muller, H., Poore, R.Z., Porter, S.C., Seret, G., Shackleton, N.J., Turner, C., Tzedakis, P.C.,
564 Winograd, I.J., 2002. Last interglacial climates. *Quatern. Res.* 58, 2-13. doi: 10.1006/qres.2002.2316
- 565 Lydolph, P.E., 1977. *Geography of the USSR*. Elsevier, The Hague.
- 566 Mackay, A., 2007. The paleoclimatology of Lake Baikal: A diatom synthesis and prospectus. *Earth*
567 *Science Reviews* 82, 181-215
- 568 Mackay, A.W., Swann, G.E.A., Fagel, N., Fietz, S., Leng, M.J., Morley, D., Rioual, P., Tarasov, P.,
569 2013. Hydrological instability during the Last Interglacial in central Asia: a new diatom oxygen isotope
570 record from Lake Baikal. *Quaternary Science Reviews* 66, 45-54. doi: 10.1016/j.quascirev.2012.09.025
- 571 Martin-Jezequel, V., Hildebrand, M., Brzezinski, M.A., 2000. Silicon metabolism in diatoms:
572 Implications for growth. *J. Phycol.* 36, 821-840. doi: 10.1046/J.1529-8817.2000.00019.X
- 573 Milligan, A.J., Varela, D.E., Brzezinski, M.A., Morel, F.O.M.M., 2004. Dynamics of silicon
574 metabolism and silicon isotopic discrimination in a marine diatom as a function of pCO₂. *Limnol.*
575 *Oceanogr.* 49, 322-329

- 576 Morley, D.W., Leng, M.J., Mackay, A.W., Sloane, H.J., Rioual, P., Sturm, M., 2004. Cleaning of lake
577 sediment samples for diatom oxygen isotope analysis. *J. Paleolimnol.* 31, 391-401
- 578 Opfergelt, S., Eiriksdottir, E.S., Burton, K.W., Einarsson, A., Siebert, C., Gislason, S.R., Halliday,
579 A.N., 2011. Quantifying the impact of freshwater diatom productivity on silicon isotopes and silicon
580 fluxes: Lake Myvatn, Iceland. *Earth. Planet. Sci. Lett.* 305, 73-82. doi: 10.1016/j.epsl.2011.02.043
- 581 Oppo, D.W., McManus, J.F., Cullen, J.L., 2006. Evolution and demise of the Last Interglacial warmth
582 in the subpolar North Atlantic. *Quaternary Science Reviews* 25, 3268-3277. doi:
583 10.1016/j.quascirev.2006.07.006
- 584 Panizzo, V.N., Roberts, S., Swann, G.A.A., McGowan, S., Mackay, A.W., Vologina, E., Pashley, V.,
585 Horstwood, M.S.A., In review. Spatial differences in dissolved silicon utilisation in Lake Baikal,
586 Siberia: disentangling the effects of high diatom biomass events and eutrophication. *Limnol. Oceanogr.*
- 587 Panizzo, V.N., Swann, G.E., Mackay, A.W., Vologina, E.G., Pashley, V.H., Horstwood, M.S.A., 2017.
588 Constraining modern-day silicon cycling in Lake Baikal. *Global Biogeochem. Cycles* 2017, 556-574.
589 doi: 10.1002/2016GB005518
- 590 Panizzo, V.N., Swann, G.E.A., Mackay, A.W., Vologina, E., Sturm, M., Pashley, V., Horstwood,
591 M.S.A., 2016. Insights into the transfer of silicon isotopes into the sediment record. *Biogeosciences* 13,
592 147-157. doi: 10.5194/bg-13-147-2016
- 593 Past Interglacials Working Group of PAGES., 2016. Interglacials of the last 800,000 years. 54, 162-
594 219. doi:10.1002/2015RG000482
- 595 Popovskaya, G.I., 2000. Ecological monitoring of phytoplankton in Lake Baikal. *Aquat. Ecosyst.*
596 *Health Manage.* 3, 215-225
- 597 Popovskaya, G.I., Usoltseva, M.V., Domysheva, V.M., Sakirko, M.V., Blinov, V.V., Khodzher, T.V.,
598 2015. The Spring Phytoplankton in the Pelagic Zone of Lake Baikal During 2007-2011. *Geogr. Natural*
599 *Resources* 36, 253-262. doi: 10.1134/s1875372815030051
- 600 Prokopenko, A.A., Hinnov, L.A., Williams, D.F., Kuzmin, M.I., 2006. Orbital forcing of continental
601 climate during the Pleistocene: a complete astronomically tuned climatic record from Lake Baikal, SE
602 Siberia. *Quaternary Science Reviews* 25, 3431-3457. doi: 10.1016/j.quascirev.2006.10.002
- 603 Prokopenko, A.A., Karabanov, E.B., Williams, D.F., Kuzmin, M.I., Shackleton, N.J., Crowhurst, S.J.,
604 Peck, J.A., Gvozdkov, A.N., King, J.W., 2001. Biogenic silica record of the Lake Baikal response to
605 climatic forcing during the Brunhes. *Quatern. Res.* 55, 123-132. doi: 10.1006/qres.2000.2212
- 606 Railsback, L.B., Gibbard, P.L., Head, M.J., Voarintsoa, N.R.G., Toucanne, S., 2015. An optimized
607 scheme of lettered marine isotope substages for the last 1.0 million years, and the climatostratigraphic
608 nature of isotope stages and substages. *Quaternary Science Reviews* 111, 94-106. doi:
609 10.1016/j.quascirev.2015.01.012
- 610 Reynolds, B.C., Aggarwal, J., Andre, L., Baxter, D., Beucher, C., Brzezinski, M.A., Engström, E.,
611 Georg, R.B., Land, M., Leng, M.J., Opfergelt, S., Rodushkin, I., Sloane, H., van den Boorn, S.H.J.M.,
612 Vroon, P.Z., Cardinal, D., 2007. An inter-laboratory comparison of Si isotope reference materials. *J.*
613 *Anal. At. Spectrom.* 22, 561-568
- 614 Rioual, P., Mackay, A.W., 2005. A diatom record of centennial resolution for the Kazantsevo
615 Interglacial stage in Lake Baikal (Siberia). *Global Planet. Change* 46, 199-219. doi:
616 10.1016/j.gloplacha.2004.08.002
- 617 Ryves, D.B., Jewson, D.H., Sturm, M., Battarbee, R.W., Flower, R.J., Mackay, A.W., Granin, N.G.,
618 2003. Quantitative and qualitative relationships between planktonic diatom communities and diatom
619 assemblages in sedimenting material and surface sediments in Lake Baikal, Siberia. *Limnol. Oceanogr.*
620 48, 1643-1661

- 621 Shimaraev, M.N., Granin, N.G., Zhdanov, A.A., 1993. Deep ventilation of Lake Baikal waters due to
622 spring thermal bars. *Limnological and Oceanography* 38, 1068-1072
- 623 Short, D.A., Mengel, J.G., Crowley, T.J., Hyde, W.T., North, G.R., 1991. Filtering of Milankovitch
624 Cycles by Earths Geography. *Quatern. Res.* 35, 157-173. doi: 10.1016/0033-5894(91)90064-C
- 625 Stumm, W., Wollast, R., 1990. Coordination chemistry of weathering: kinetics of the surface-
626 controlled dissolution of oxide minerals. *Review of Geophysics* 28, 53-69
- 627 Sun, X.L., Andersson, P.S., Humborg, C., Pastuszak, M., Morth, C.M., 2013. Silicon isotope
628 enrichment in diatoms during nutrient-limited blooms in a eutrophied river system. *Journal of*
629 *Geochemical Exploration* 132, 173-180. doi: 10.1016/J.Gexplo.2013.06.014
- 630 Sutton, J.N., Varela, D.E., Brzezinski, M.A., Beucher, C.P., 2013. Species-dependent silicon isotope
631 fractionation by marine diatoms. *Geochim. Cosmochim. Acta* 104, 300-309. doi:
632 10.1016/J.Gca.2012.10.057
- 633 Tarasov, P., Bezrukova, E., Karabanov, E., Nakagawa, T., Wagner, M., Kulagina, N., Letunova, P.,
634 Abzaeva, A., Granoszewski, W., Riedel, F., 2007. Vegetation and climate dynamics during the
635 Holocene and Eemian interglacials derived from Lake Baikal pollen records. *Palaeogeography,*
636 *Palaeoclimatology, Palaeoecology* 252, 440-457. doi: 10.1016/j.palaeo.2007.05.002
- 637 Tarasov, P., Granoszewski, W., Berzukova, Y.V., Brewer, S., Nita, M., Abzaeva, A., Oberhaensli, H.,
638 2005. Quantitative reconstruction of the Last Interglacial climate based on the pollen record from Lake
639 Baikal, Russia. *Clim. Dyn.* 25, 625-637
- 640 Varela, D.E., Pride, C.J., Brzezinski, M.A., 2004. Biological fractionation of silicon isotopes in
641 Southern Ocean surface waters. *Global Biogeochem. Cycles* 18. doi: 10.1029/2003gb002140
642
- 643 Velichko, A.A., Borisova, O.K., Gurtovaya, Y.Y., Zelikson, E.M., 1991. Climatic rhythm of the last
644 interglacial in northern Eurasia. *Quaternary International* 10-12, 191-213
- 645 Williams, D.F., Kuzmin, M.I., Prokopenko, A.A., Karabanov, E.B., Khursevich, G.K., Bezrukova,
646 E.V., 2001. The Lake Baikal drilling projects in the context of a global lake drilling initiative.
647 *Quaternary International* 80-1, 3-18. doi: 10.1016/S1040-6182(01)00015-5
648
- 649